

Janina Repelewska-Pękalowa

Kazimierz Pękala

Piotr Zagórski

Józef Superson

5.3. Permafrost and periglacial processes

The NW part of Wedel Jarlsberg Land lies within the range of continuous permafrost whose thickness in Spitsbergen is between 200 and 450 m (Liestøl 1976; Landvik *et al.* 1988; Kristensen 1988; Åkerman 1993). The weather conditions during the few months of the polar summer, with temperatures above zero, are conducive to the thawing of the ground and formation of the permafrost active layer. The research problems addressed by the Maria Curie-Skłodowska University (UMCS) Polar Expeditions included the dynamics and depth of permafrost thawing in the summer as well as the identification of local factors determining the process.

The thickness of the permafrost active layer was measured during the UMCS Expeditions, starting from 1986, using three methods: (1) probing with a steel rod, (2) Danilin's frostmeter and (3) based on identifying the location of the 0°C isotherm in the ground: based on ground thermometer readings in the first years and after 1999, using a temperature gradient probe. The measurement points, representative of the tundra environment, were located within the Calypsostranda coastal plain, consisting of a system of raised marine terraces adjoining the forefields of the Scottbreen and Renardbreen (Zagórski 2002, 2007c) (see: Fig. 1.2, Appendix 2). The sites of permafrost active layer thickness measurements differed with regard to the degree of ground water mobility, vegetation cover, aspect and terrain inclination (Repelewska-Pękalowa *et al.* 1988; Repelewska-Pękalowa 2004; Pękala & Repelewska-Pękalowa 2004).

The maximum extent of the summer thaw varied considerably: from 40 cm to more than 225 cm (Table 5.3.1). The shallowness thaw was recorded in a site with stagnant surface water (a small, shallow tundra lake), while the deepest thaw was found in places where the movement of ground water – a heat-transfer medium – occurred. In the case of sloping surfaces, a significant role was played by aspect, type of ground and degree of its humidity. Various aspects of this problem have been addressed in numerous studies (e.g. Repelewska-Pękalowa *et al.* 1987a; Repelewska-Pękalowa & Magierski 1989; Repelewska-Pękalowa & Paszczyk 1990). They were also presented at international conferences dedicated to permafrost in: Trondheim (1988), Pekin (1993), Zurich (2003) and Potsdam (2005) (e.g. Gluza & Repelewska 1988; Gluza *et al.* 1988; Repelewska-Pękalowa & Gluza 1988b; Bartoszewski *et al.* 1993; Christian-

5.3. Permafrost and periglacial processes

sen *et al.* 2003; Repelewska-Pękalowa & Pękalowa 2003, 2004a) and at conferences in Poland (e.g. Repelewska-Pękalowa *et al.* 1988; Repelewska-Pękalowa & Pękalowa 2004b, 2006, 2007).

The results of the permafrost active layer thickness measurements conducted during the UMCS polar expeditions, recognised as representative of areas under the influence of the northern Atlantic, were included (as Site P1 – Calypsostranda) in the international CALM program (Circumpolar Active Layer Monitoring). The program's goal was to collect and make available the results of studies in over 200 areas on both hemispheres. These data can be used to create models of the functioning and response of permafrost to global and regional climate changes (Brown *et al.* 2000; Repelewska-Pękalowa 2002; Christiansen *et al.* 2003; Repelewska-Pękalowa & Pękalowa 2004ab, 2007; Marsz *et al.* 2011) (Fig. 5.3.1).

Table 5.3.1. Summer thawing of permafrost active layer in different points at Calypsostranda in the period 1986-2009 (maximum values in cm).

Year	Point / Site									
	1	2	3	4	5	6	I	II	III	IV
1986	90	125	120	-	60	-	120	-	145	122
1987	111	175	175	175	68	124	124	150	165	130
1988	108	163	168	193	70	148	121	180	177	135
1989	145	165	157	180	83	155	135	160	186	139
1990	130	165	165	165	56	137	118	135	170	122
1991	127	148	163	170	75	155	141	150	165	121
1992	140	170	165	180	70	145	140	180	155	125
1993	112	180	180	196	70	165	130	180	180	140
1995	125	176	180	174	68	174	135	170	160	140
1996	125	154	178	168	65	151	132	160	151	128
1998	130	124	121	170	75	150	-	-	160	-
2000	108	175	155	130	45	145	126	135	160	150
2001	116	131	180	165	73	154	150	170	132	155
2002	130	155	170	154	81	150	139	160	150	-
2005	150	225	220	210	115	160	157	195	200	145
2006	159	>217	>217	>217	180	178	215	>220	200	218
2007	166	>217	>217	>217	176	187	>217	>217	>217	>217
2008	156	>205	>217	>217	155	172	195	>205	>205	>205
2009	151	>203	>203	>203	>203	>203	>203	>203	>203	>203
2011	169	>202	>202	>202	>202	>202	>202	>202	>202	>202
2012	164	>202	>202	>202	>202	>202	>202	>202	>202	>202

Points 1-5 are located on north-south and west-east transects on raised marine terrace, 20-30 m a.s.l.: 1- a flat marine terrace built of sands and gravels, sparse tundra vegetation; 2- patterned ground with running water within sandy-gravelly surface material, mosses on the peat layer; 3- patterned ground, running water in the surficial material, formed of sands and coarse gravels, absence of vegetation; 4- small stream, between points 2 and 4, gravelly sandy cover, absence of vegetation; 5- peat within a shallow lake; 6- sandy beach, absence of vegetation: I- northerly slope of Tyvjobekken valley, tundra; II- southerly slope of Tyvjobekken valley, tundra; III- dead cliff, easterly orientation; IV- westerly slope of Reindyrbekken valley, tundra. In the summer seasons of 2006-2012 measurements made by members of UMCS Polar Expeditions (Raport: Department of Geomorphology UMCS).

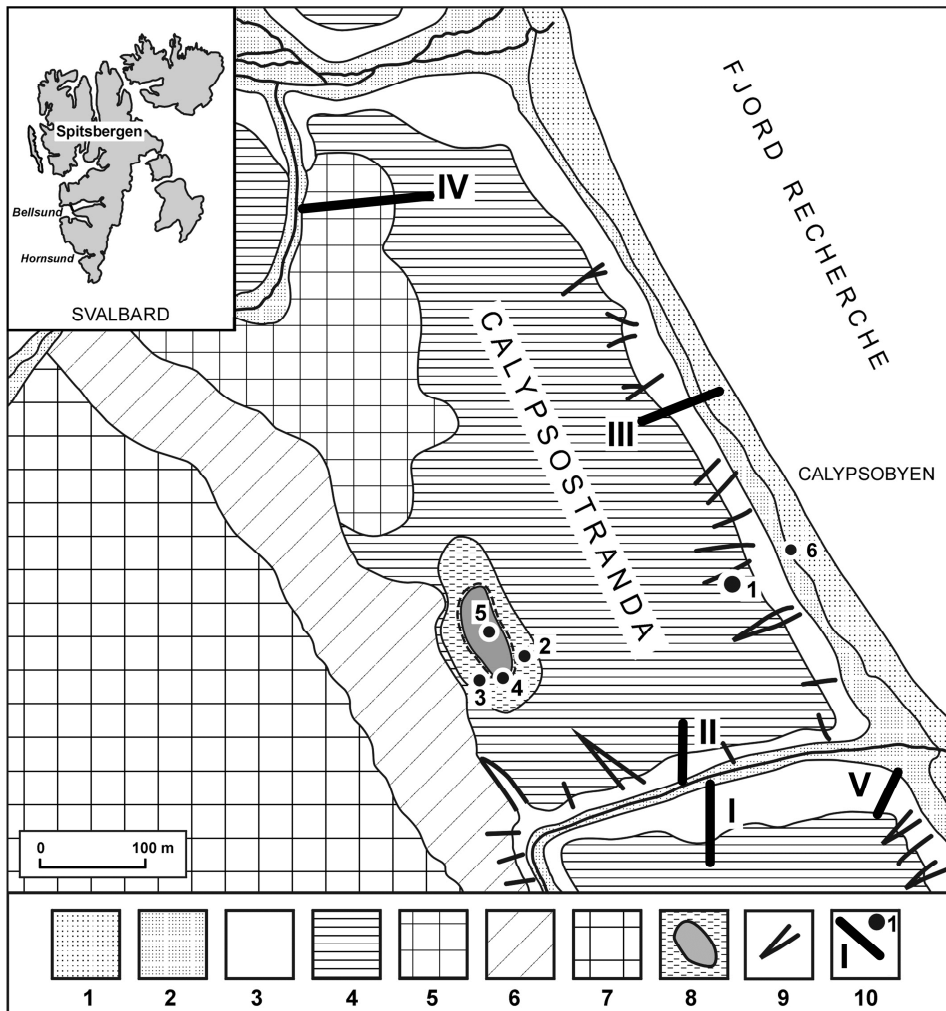


Fig. 5.3.1. Main sets of forms and location of measurement points of active layer of permafrost (Repelewska-Pękalowa & Pękalowa, 2003): 1- beach, 2- floors of valleys and zones of alluvial cones at the cliff base, 3- cliff and erosive edges of valleys, 4- dry surfaces of marine terraces, 5- zones of active solifluction, 6- periodically wet terraces aggradated with alluvial cones, 7- slopes and high marine terraces converted by weathering, cryo-planation and erosive processes, 8- seasonal lake, 9- erosive dissection, 10- measurement points and profiles.

The dynamics of the permafrost active layer and periglacial processes depends mainly on climate conditions (Christiansen *et al.* 2003; Repelewska-Pękalowa & Pękalowa 2003, 2004a; Repelewska-Pękalowa 2004). A comparison of the extent of the summer thawing of permafrost in Spitsbergen with changes in atmospheric circulation and temperatures of the sea indicates a strong influence of the cumulative air temperature between February and August, particularly in May and June (Marsz *et al.* 2011). It remains under a strong influence of the surface temperature of the Greenland Sea where the West Spitsbergen Current flows. The present studies indicate that from 1986 to 2002, despite the considerable year-to-year variability of the maximum thickness of the

permafrost active layer, its changes occurred without any specific trend. It was only in 2002-2004 that a very strong, clear tendency was observed for the permafrost active layer thickness to increase in the period of the maximum extent of the summer thaw (Marsz *et al.* 2011). The maximum acceleration of the thawing rate on Calypsostranda was observed in the years 2005-2006 while in 2007 it suddenly slowed down. The sudden increase of the active layer thickness recorded on Calypsostranda in the years 2005-2006 is consistent with other observations of permafrost behaviour in Spitsbergen. According to Isaksen *et al.* (2007), it is linked to the occurrence of highly abnormal above-zero temperatures in Spitsbergen in the winter of 2005/2006 and spring of 2006. The variability of the permafrost active layer is also determined, to a certain extent, by local factors such as terrain configuration and aspect, vegetation cover as well as the kind and degree of ground-water mobility, which was already mentioned by Repelewska-Pękalowa & Gluza (1988ab), Brown *et al.* (2000), Christiansen *et al.* (2003) or Repelewska-Pękalowa & Pękala (2003, 2004a).

The landforms, geological structure – the type of surface sediments in particular, the presence of surface waters and their circulation within the permafrost active layer are conducive to the development of periglacial processes such as frost weathering, solifluction, washing, mud flow, landslides, ice segregation and frost heaving and rill erosion. Structured ground, veins, lenses and ice wedges as well as pingos and palsas with ice cores are formed. Periglacial processes and forms investigated during UMCS Polar Expeditions were the subject of numerous publications (e.g. Dzierżek & Nitychoruk 1987ac; Repelewska-Pękalowa 1987, 1996; Szczęsny 1987; Repelewska-Pękalowa & Pękala 1993; Pękala & Repelewska-Pękalowa 2004, 2005, 2007a; Superson & Zagórski 2008).

The leading role among periglacial processes occurring in central Spitsbergen is played by **solifluction** (Jahn 1970). This slow movement of thawed, humid layer of ground on a frozen substratum occurs on sloping surfaces. Solifluction processes modelling the middle and lower sections of slopes are characterised by increasing activity. In some cases they take the form of tongues, while in other cases it is the creeping of the whole width of permafrost active layer while a solifluction terrace forms at the base of the slope (Figs. 5.3.2 and 5.3.3; Photo 5.3.1AB). Slope processes and forms of this type are linked to the increased thickness of the active layer as a result of the movement of water in the covers (Repelewska-Pękalowa *et al.* 1988; Repelewska-Pękalowa 2004).

The solifluction movement data were obtained for two periods: 1987-1991 and 2006-2009. In both periods, the investigation was concerned with: (I) the side of the Tyvjobekken valley with N aspect and mean inclination of 8%, (II) the side of the Tyvjobekken valley with S aspect and mean inclination of 23%, (III) the side of a dead cliff of Calypsostranda with E aspect and mean inclination of 19%, the side of the Rensdyrbekken (Reindeer stream) valley with W aspect and mean inclination of 8%. In addition, in the years 2006-2009, measurements were also conducted on the slope

at the mouth of the Tyvjobekken valley with NE aspect and mean inclination of 10% (Fig. 5.3.4). The methods used to obtain data for each of these periods differed, and the precise location of the measurement points was different; hence a straightforward comparison of the results is impossible. However, the general trend of changes occurring within the investigated slopes can be identified based on these data.

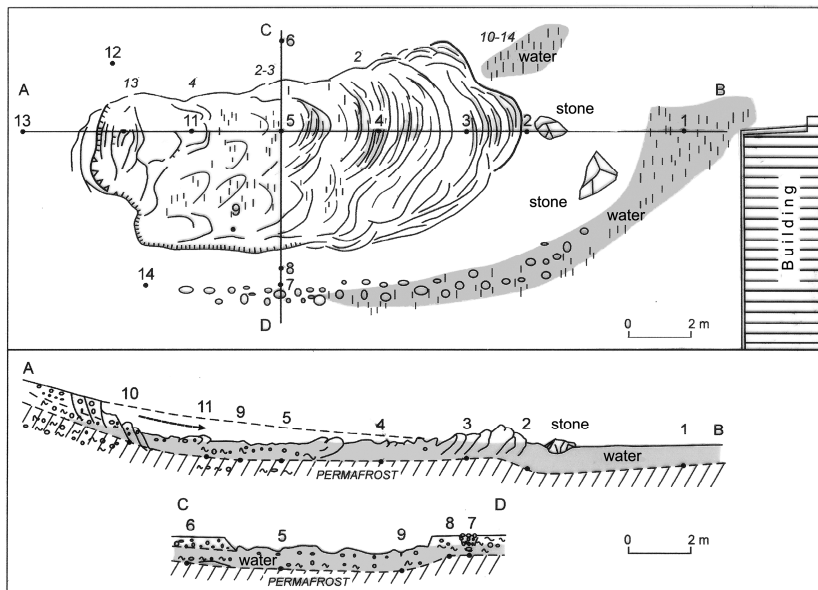


Fig. 5.3.2. Plan and profiles of mudflow on the slope of dead cliff of terrace 20-25 m a.s.l., Calypsobyen (Pękala 2004).

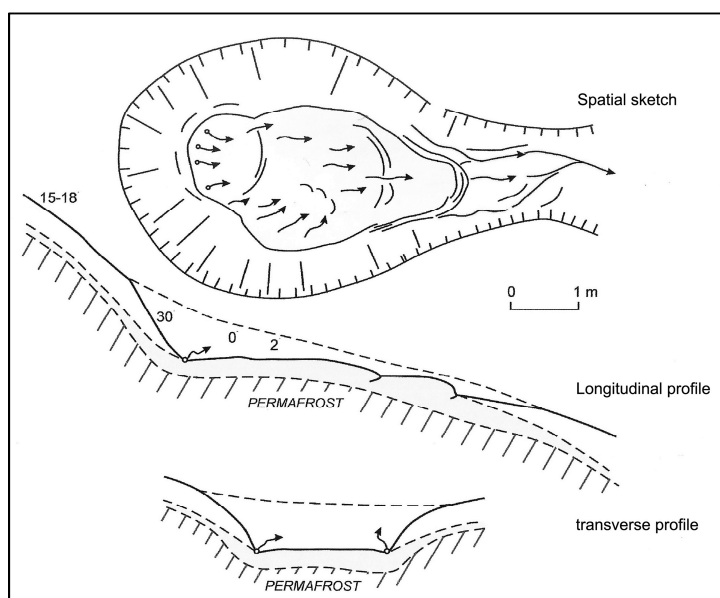


Fig. 5.3.3. Plan and profiles of bog cirque with solifluction tongue (Pękala 2004).

5.3. Permafrost and periglacial processes

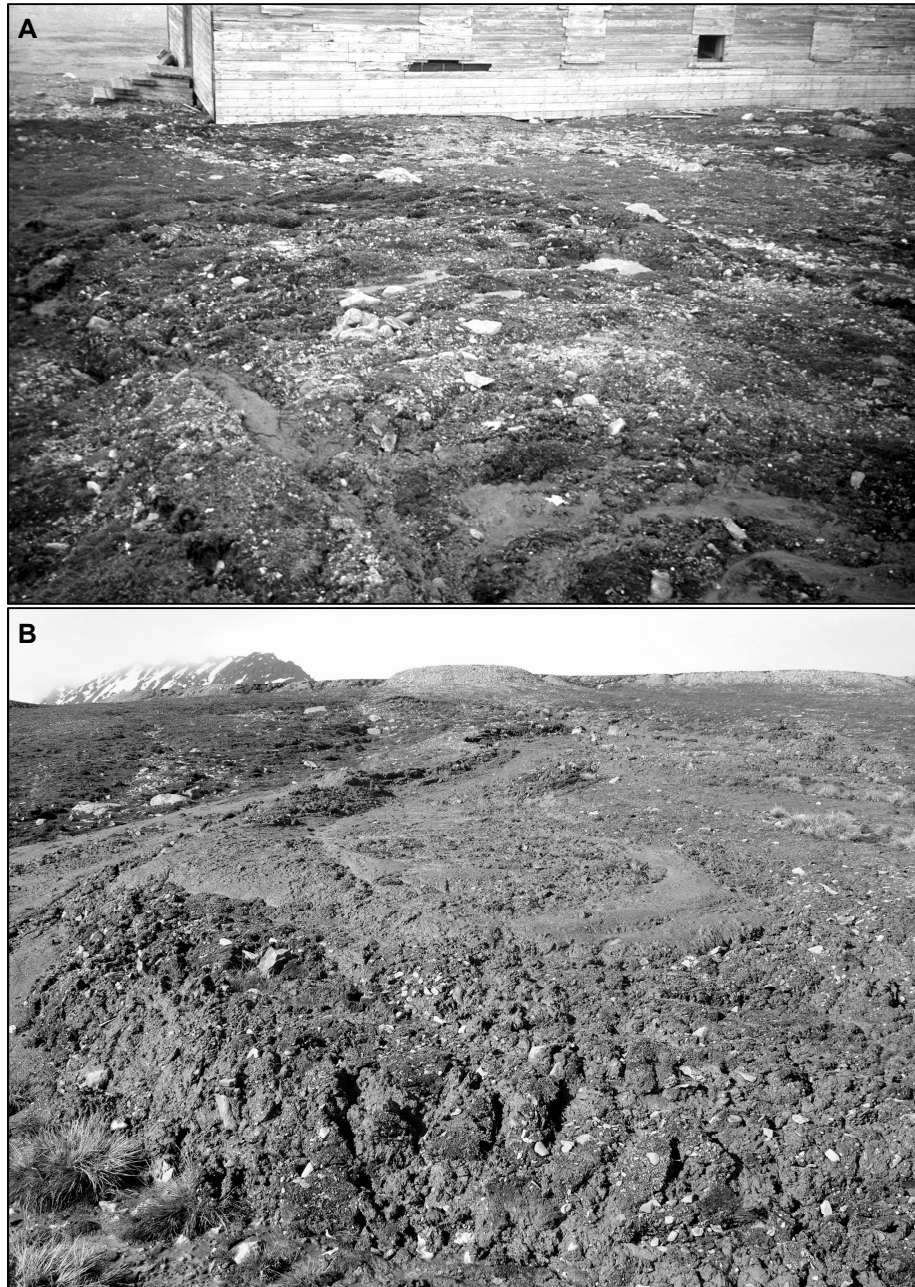


Photo 5.3.1. A- mudflow on the slope above the building – Calypsobyen (Photo K. Pękala 2005), B- of bog cirque with solifluction tongue (Photo P. Zagórski 2010).

In the period 1987-1991, solifluction movement was measured using metal surveying tape and metal pins installed at selected points. The rate of movement was found to vary depending on the inclination and aspect (Table 5.3.2).

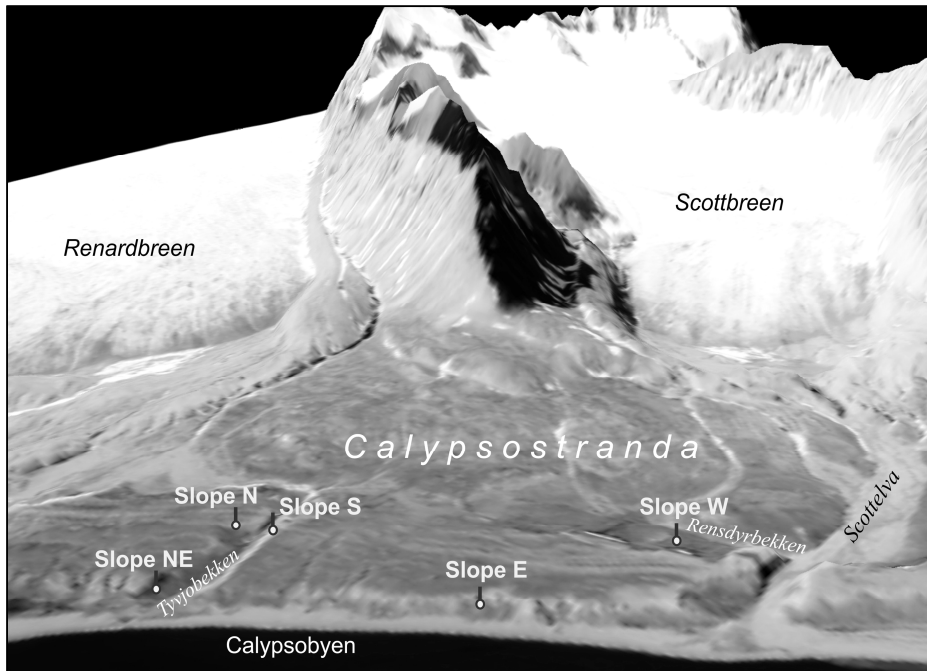


Fig. 5.3.4. Location of studied slopes (DEM, Zagórski 2002).

Table 5.3.2. Solifluction rate in Calypsostranda region on the slope with different aspects and different slope sections in the 1987-1991 period (Repelewska-Pękalowa & Pękala 1993)

Slope section	N (I)	S (II)	E (III)	W (IV)	Mean
	[cm·a ⁻¹]				
Upper	3.0	3.0	16.0	4.0	6.5
Middle	4.0	40.0	3.0	8.0	13.75
Lower	12.0	2.0	2.0	17.0	8.25
Mean	6.4	15.0	7.0	9.6	9.5

N (I) – northerly slope of Tyvjobekken valley, tundra; S (II) – southerly slope of Tyvjobekken valley, tundra; E (III) – dead cliff, easterly orientation; W (IV) – westerly slope of Rensdyrbekken valley, tundra.

The highest rate, $40 \text{ cm} \cdot \text{a}^{-1}$, was recorded in the middle section of the slope with S aspect, a result of ground temperature frequently passing the 0°C mark. Quite a high rate was also recorded on the W-aspect slope ($17 \text{ cm} \cdot \text{a}^{-1}$), implying a rather long presence of the snow cover followed by a strong humidification of the ground. The mean solifluction rate was $9.5 \text{ cm} \cdot \text{a}^{-1}$. A similar rate for Spitsbergen ($5-12 \text{ cm} \cdot \text{a}^{-1}$) is provided by Jahn (1967). By comparison, the rate of solifluction movement measured in other areas was: $0.9-3.7 \text{ cm} \cdot \text{a}^{-1}$ in Greenland (Washburn 1967), $0.8-2.7 \text{ cm} \cdot \text{a}^{-1}$ in the Canadian Arctic (Price 1974), and $2 \text{ cm} \cdot \text{a}^{-1}$ in Kärkevagge (Sweden) (Rapp 1960).

In the second period, 2006-2009, the movements of the solifluction cover were measured by means of GPS surveying receivers (Leica, system 500). In the profiles

mentioned above, metal pins (E slope) and wooden pegs (the other profiles) were installed. The static method was used in GPS measurements (post-processing calculation), with 15 to 20-minute observation sessions. The results were adjusted and correlated with the reference station (CALY Point) installed at the UMCS Polar Station at Calypsobyen. The observations were repeated each year at the end of the season (August/September), in the period of the maximum thickness of the permafrost active layer. The measurement error was $\pm 1\text{-}2$ cm. The results obtained indicate that:

1) eastern exposure slope (E slope): the greatest solifluction movement occurred in the upper section of the slope, at the base of its upper recess (23.1 cm, $7.7 \text{ cm}\cdot\text{a}^{-1}$) and the lower section of the slope where impermeable marine clay outcrops occur (21.3 cm, $7.1 \text{ cm}\cdot\text{a}^{-1}$) (Fig. 5.3.5, Photo 5.3.2A);

2) western exposure slope (W slope): ground movement below the upper recess of the slope was similar along the entire profile and ranged from 10.9–15.7 cm ($3.6\text{--}5.2 \text{ cm}\cdot\text{a}^{-1}$) in the upper section, to 14.5–17.1 cm ($4.8\text{--}5.7 \text{ cm}\cdot\text{a}^{-1}$) in the lower section (Fig. 5.3.6, Photo 5.3.2B);

3) northern exposure slope (N slope): the upper section of the slope was characterised by high stability while in the lower section, at outcrops of impermeable marine clay, the solifluction movement of the covers reached a maximum of 17.6 cm ($5.9 \text{ cm}\cdot\text{a}^{-1}$) and 12.8 cm ($4.3 \text{ cm}\cdot\text{a}^{-1}$), and a solifluction lobe formed (Fig. 5.3.7, Photo 5.3.3A);

4) southern exposure slope (S slope): the upper, dried-out (marine gravels) section of the slope was stable despite its steepness, while in the lower section, where glacial till and marine clay occurred, solifluction lobes developed (in the nival niche), as a result of which the ground moved by 131–528 cm (Fig. 5.3.8, Photo 5.3.3B);

5) north-eastern exposure slope (NE slope): the maximum solifluction movement of the covers occurred in the middle, humid section (21.8 cm, $7.3 \text{ cm}\cdot\text{a}^{-1}$) and the lower section of the slope, where solifluction lobes developed (15.3 cm, $5.1 \text{ cm}\cdot\text{a}^{-1}$) (Fig. 5.3.9, Photo 5.3.4).

Taking into account all measurement points for the particular slopes, the mean values of solifluction movement in the 2006–2009 period were respectively: E slope: 14.4 cm ($4.8 \text{ cm}\cdot\text{a}^{-1}$), W slope: 14.1 cm ($4.7 \text{ cm}\cdot\text{a}^{-1}$), N slope: 6.2 cm ($2.1 \text{ cm}\cdot\text{a}^{-1}$), S slope: 159.8 cm ($53.3 \text{ cm}\cdot\text{a}^{-1}$), NE slope: 13.1 cm ($4.3 \text{ cm}\cdot\text{a}^{-1}$).

The measurements revealed a general increase in the volume of solifluction movement from the end of the 1990s. It is closely related to the increasing thickness of the permafrost active layer, determined by climate changes, as it has been mentioned above. The morphological result was the formation of niches, cirques and basins, mud and debris tongues as well as several landslide forms on relatively gentle slopes (with an inclination up to 10°) that had been regarded as stable until then. The emergence of such forms posed a threat to buildings belonging to a skansen of early twentieth-century industrial architecture in Calypsobyen (Repelewska-Pękalowa & Pękala 1993) (Fig. 5.3.2, Photo 5.3.1)

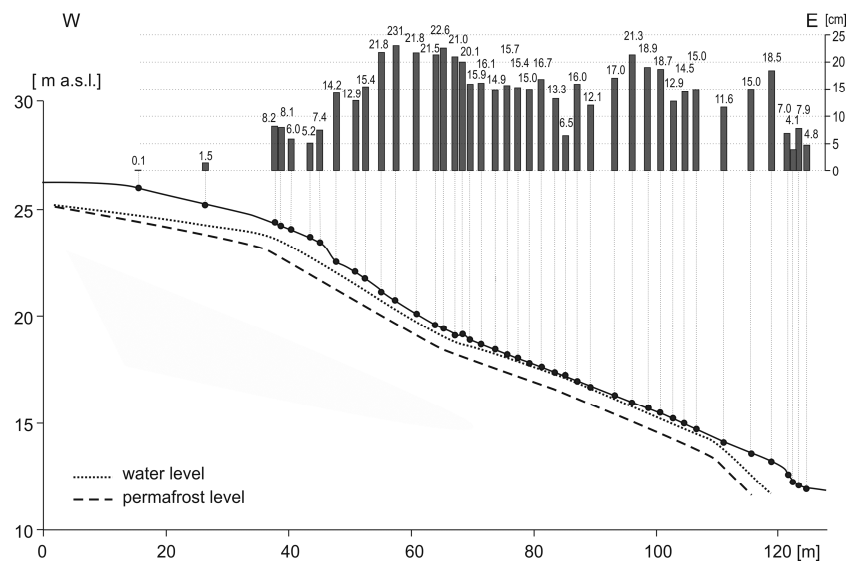


Fig. 5.3.5. The moving the solifluction cover on the E slope in 2006-2009 period.

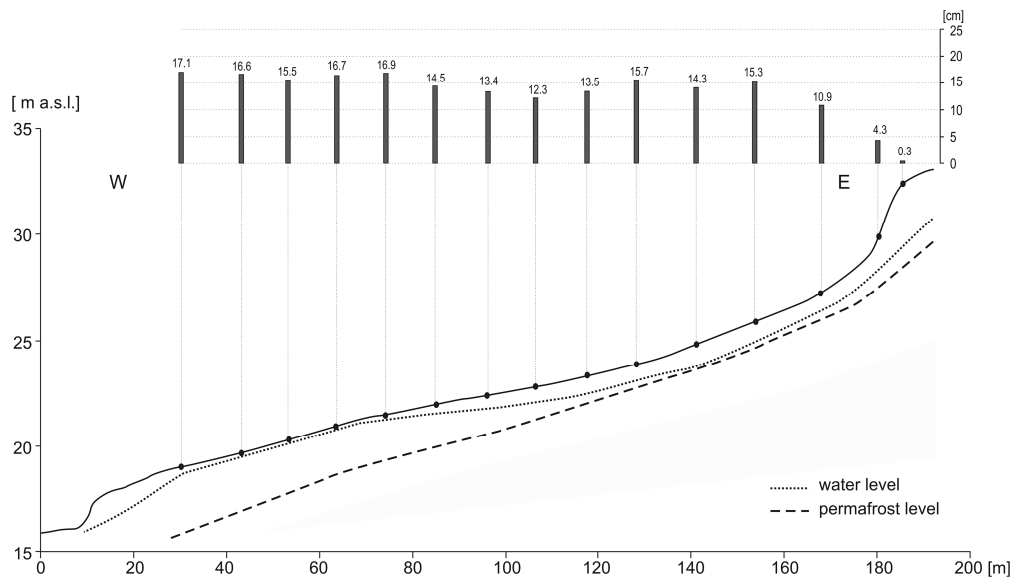


Fig. 5.3.6. The moving the solifluction cover on the W slope in 2006-2009 period.

5.3. Permafrost and periglacial processes

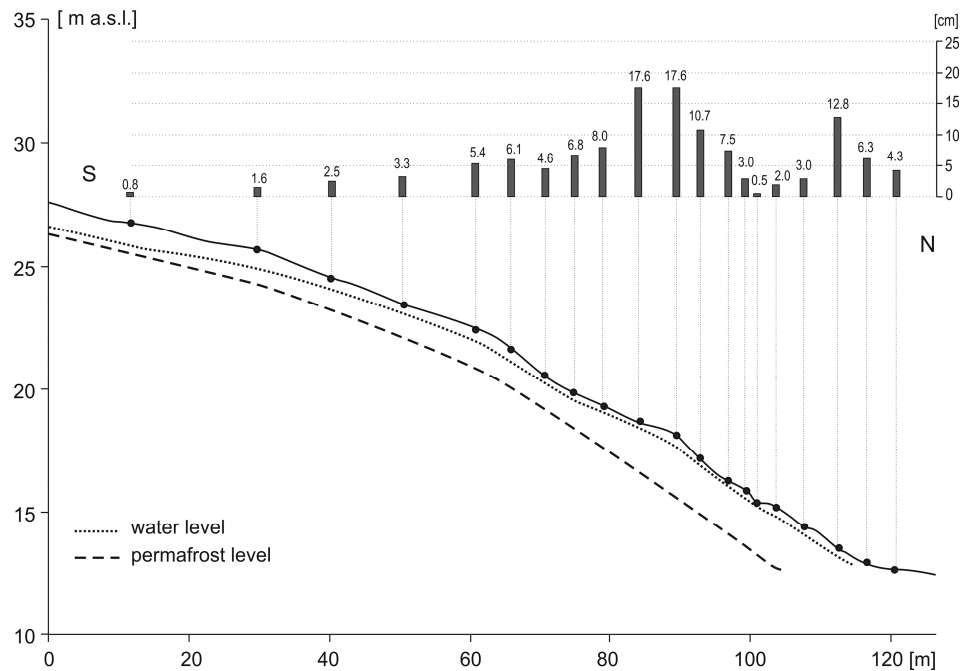


Fig. 5.3.7. The moving the solifluction cover on the N slope in 2006-2009 period.

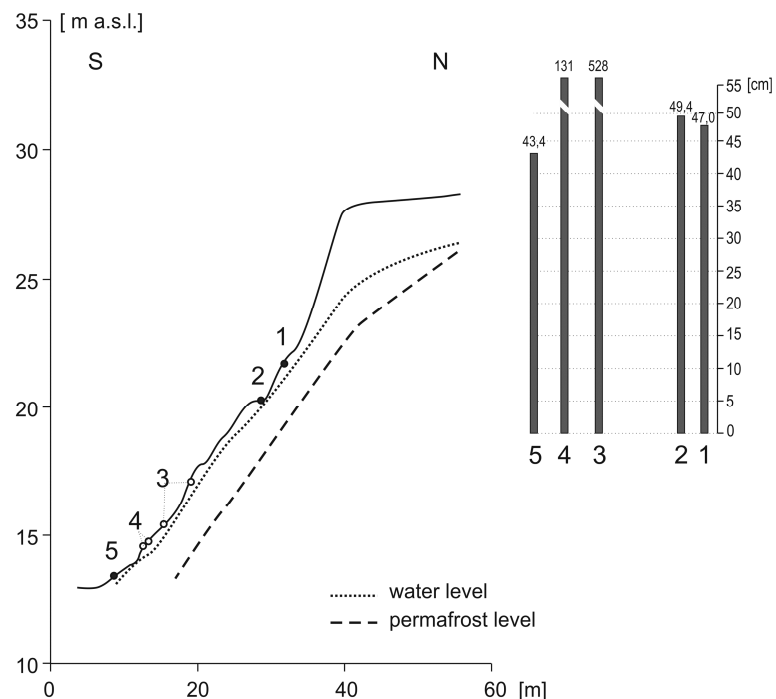


Fig. 5.3.8. The moving the solifluction cover on the S slope in 2006-2009 period.

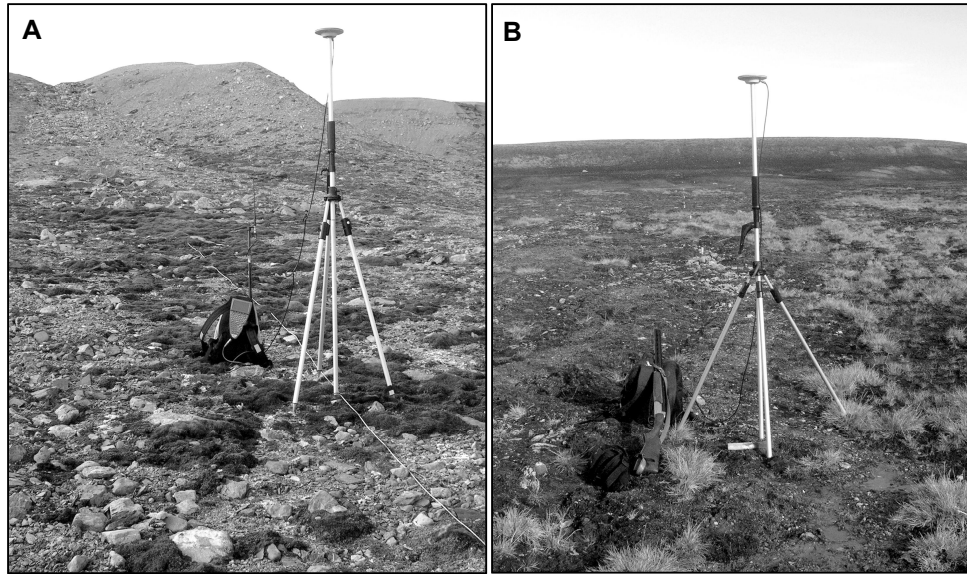


Photo 5.3.2. GPS (Leica) measurements: A- on the E slope (Photo P. Zagórski 2006), B- on the W slope (Photo P. Zagórski 2009).

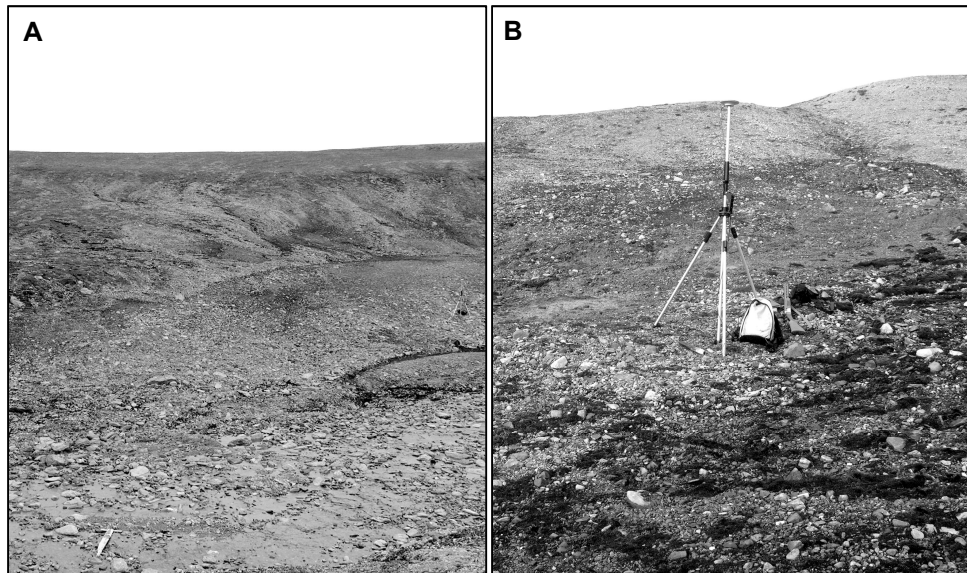


Photo 5.3.3. GPS (Leica) measurements: A- on the N slope (Photo P. Zagórski 2009); B- on the S slope (Photo P. Zagórski 2006).

The thawing of ice within the permafrost active layer, usually occurring after the thawing of the snow cover, also results in water runoff in the weathered layers and on the surface. The runoff of ice ablation water and then water from the thawing active layer, both down short and steep slopes as well as coastal plains, triggers **washing** (Photo 5.3.5AB). They can be estimated by the volume of material transported in the form of

5.3. Permafrost and periglacial processes

suspended matter by pronival streams (Photo 5.3.5B). Based on measurements conducted alongside research into chemical denudation during several summer seasons at Calypsobyen within the non-glacierised Tyvjobekken catchment, it was established that the mean washing volume was $29.5 \text{ t} \cdot \text{km}^{-2}$ (Bartoszewski & Repelewska-Pękalowa 1988b; Bartoszewski & Magierski 1989ab; Bartoszewski 1994).

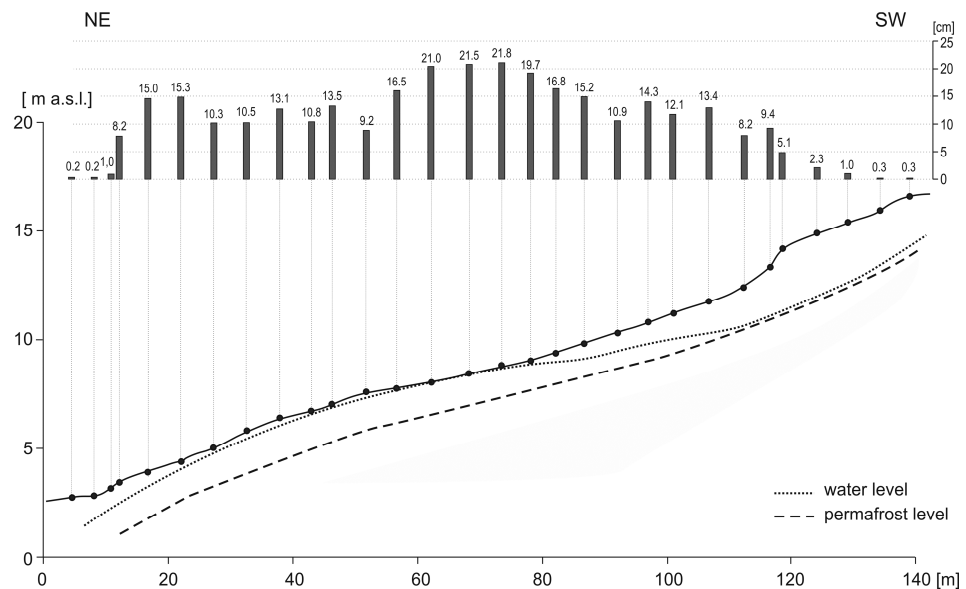


Fig. 5.3.9. The moving the solifluction cover[in cm] on the NE slope in 2006-2009 period.



Photo 5.3.4. GPS measurements on the NE slope (Photo P. Zagórski 2006).

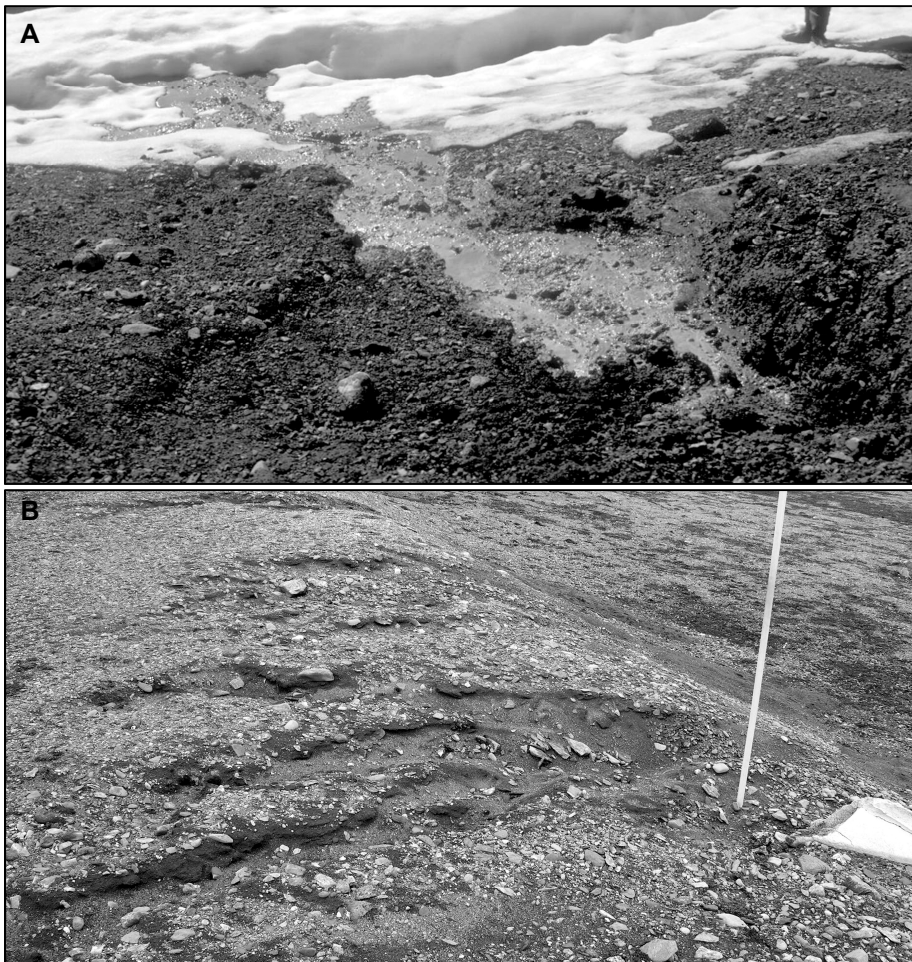


Photo 5.3.5. A,B- the washing effects near edge of raised marine terrace II, Calypsobyen (Photo A- K. Pękala; B- P. Zagórski 2006).

Within flat and humid surfaces, high activity of **ice segregation** can be observed, leading to the pushing up of stones and development of stone rings, while on dry surfaces contraction cracks and wedges are formed (Repelewska-Pękalowa 1996) (Fig. 5.3.10, Photo 5.3.6). Similar forms develop as a result of the thawing of dead-ice on the glacier forefield. Ice segregation structures and thermokarst depressions formed on the surface of the ground moraine with ice blocks and in the zone of ice-moraine belts of recessional moraines (Fig. 5.3.11).

Thermal erosion and piping result from the infiltration of precipitation water and meltwater into frost cracks and drought cracks. Thermal erosion processes were also found in tundra geoecosystems with peat vegetation (Photo 5.3.7ABC). This phenomenon was observed, among other places, on the Reinsletta, dissected by a grid of large and small tundra polygons, with aeolian covers and continuous tundra vegetation (Repelewska-Pękalowa & Pękala 1991). The morphological result of these processes is

5.3. Permafrost and periglacial processes

the formation of mini-craters, troughs and underground channels, corresponding to cryogenic systems. The collapse of the ceilings of the channels results in the formation of troughs and piping valleys (up to 23 m long, 1-4 m wide and up to 1,5 m deep), at the mouth of which alluvial fans develop. The further development of these forms is usually influenced by solifluction and solifluction/denudation valleys form in the final stage (Fig. 5.3.12).

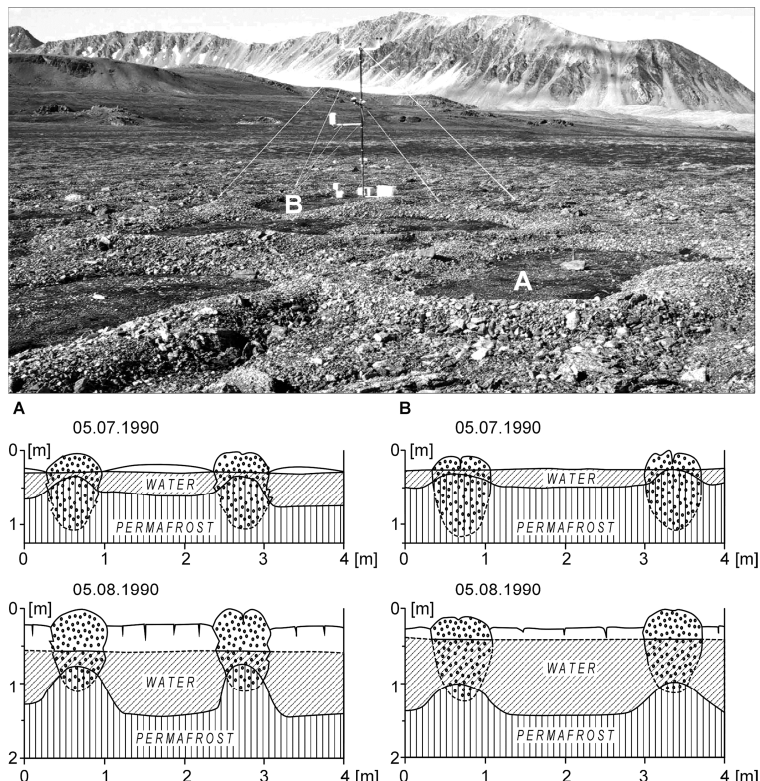


Fig. 5.3.10. Development of stone circles (after: Pękala 2004, Photo S. Bartoszewski 2002).



Photo 5.3.6. Ice segregation forms on the Capypsostranda surface near Tyvjobekken valley (Photo K. Pękala).

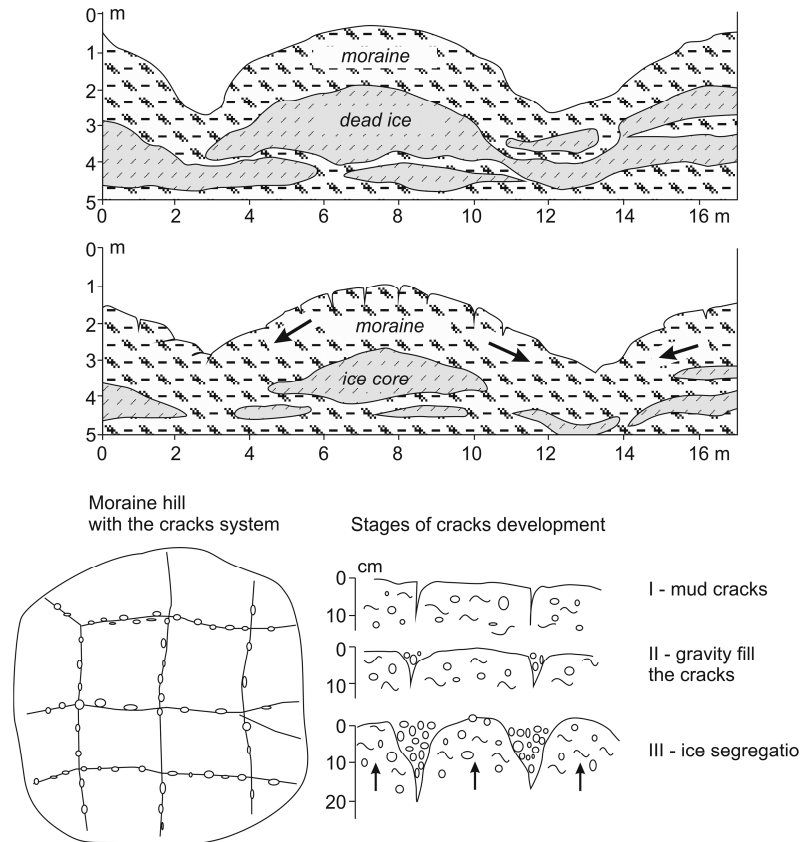


Fig. 5.3.11. Stages of cracks development on the surface of ground moraine with ice core – forefield of Renardbreen (after: Pękala 2004).

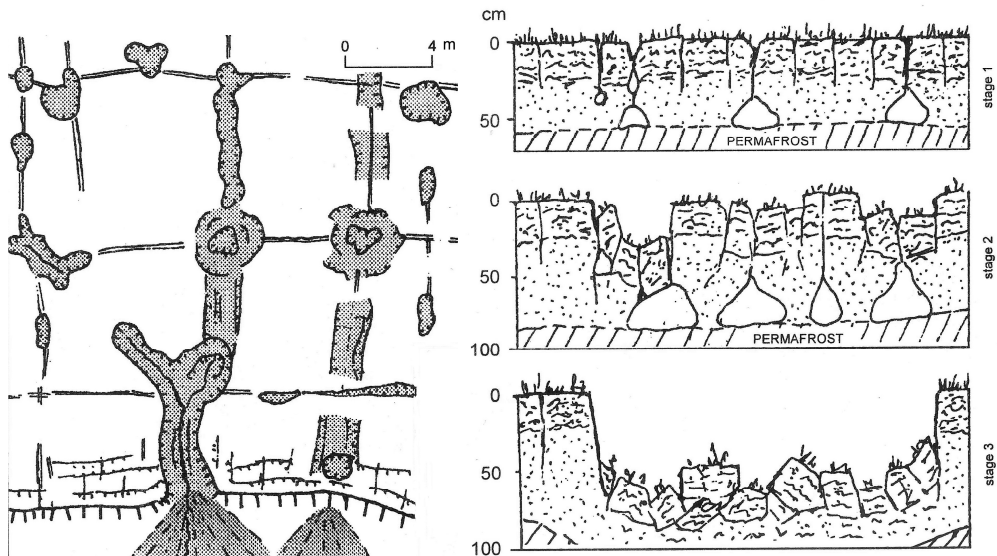


Fig. 5.3.12. Plan and development stages of piping forms (after: Repelewska-Pękalowa 1996).

5.3. Permafrost and periglacial processes



Photo 5.3.7. Examples of thermal erosion: A- near Beisoden (Photo S. Bartoszewski 2001), B- near Beisoden (Photo M. Świtoniak 2009), C- degradation of ice wedges – Reinsletta (Photo K. Pękala 2000).

Erosion forms emerge mainly within the sides of ravin valleys and edges of marine terraces (dead and present-day cliffs). They develop mainly at the beginning of the summer, under conditions of poor infiltration and shallow position of the permafrost top layer. These forms are at various stages of development: from small rills, medium-sized dissections, to large V-shaped forms (Repelewska-Pękalowa 1987, Repelewska-Pękalowa & Pękala 1991, Gawrysiak 1994ab). For example, such forms occur on the north-eastern slope of marine terrace III (25-30 m a.s.l.) to the north of Calypsobyen (Superson & Zagórski 2008) (Fig. 5.3.13, Photo 5.3.8). Erosion processes are the most intensive in the upper section of the terrace slope where several generations of dissections developed, namely (Figs. 5.3.13 and 5.3.14):

- 1) small erosion rills, sinuous and not deep (10-20 cm), about 0.5 m wide and 2 m long.
They occur where the flat terrace surface changes into the steep slope;
- 2) medium-sized erosion rills, 0.5-1.5 m deep, corresponding to thermal contraction structures. There occur erosion forms with convex slopes and flat bottoms as well as V-shaped forms;
- 3) large, V-shaped forms, 2.0-2.5 m deep, incised both into marine gravels and the underlying moraine sediments;
- 4) flat-bottomed valleys, located in the lower sections of medium-sized erosion rills and large V-shaped forms. Alluvial fans occur at the mouth of these forms, on a slightly inclined denudation surface.

Secondary erosion forms, in the form of periodic stream channels, also occur in the investigated area. They formed at the bottom of large V-shaped forms and flat-bottomed valleys as well as alluvial fans and solifluction surfaces. The channels are shallow (0.1-0.2 m deep) and paved with cobbles from a washed-out moraine. Extensive alluvial fans, consisting of fine material, currently develop where the channels open onto the marine terrace (Fig. 5.3.14). The position of small erosion rills at the edge of the terrace is not determined by thermal contraction cracks but results from the increasing inclination and transition of surface runoff into concentrated runoff, which is additionally predetermined by the absence of the vegetation cover. The uneven, undulating surface of sand-and-gravel sediments occurring at the mouth of the rills in the form of thin covers proves that these sediments were deposited on the snow and slowly subsided as the snow melted.

The formation and development of medium-sized erosion rills was largely determined by thermal contraction cracks and the lithology of the substratum. In the first stage, small erosion rills formed and became deeper as a result of the concentration of water runoff in the cracks and thermal erosion (Repelewska-Pękalowa & Pękala 1991). In some cases, erosion advanced until it reached the top layer of glacial till. Glacial till stopped the bed erosion in favour of the progressing lateral recession of the slopes of the erosion forms (Fig. 5.3.14).

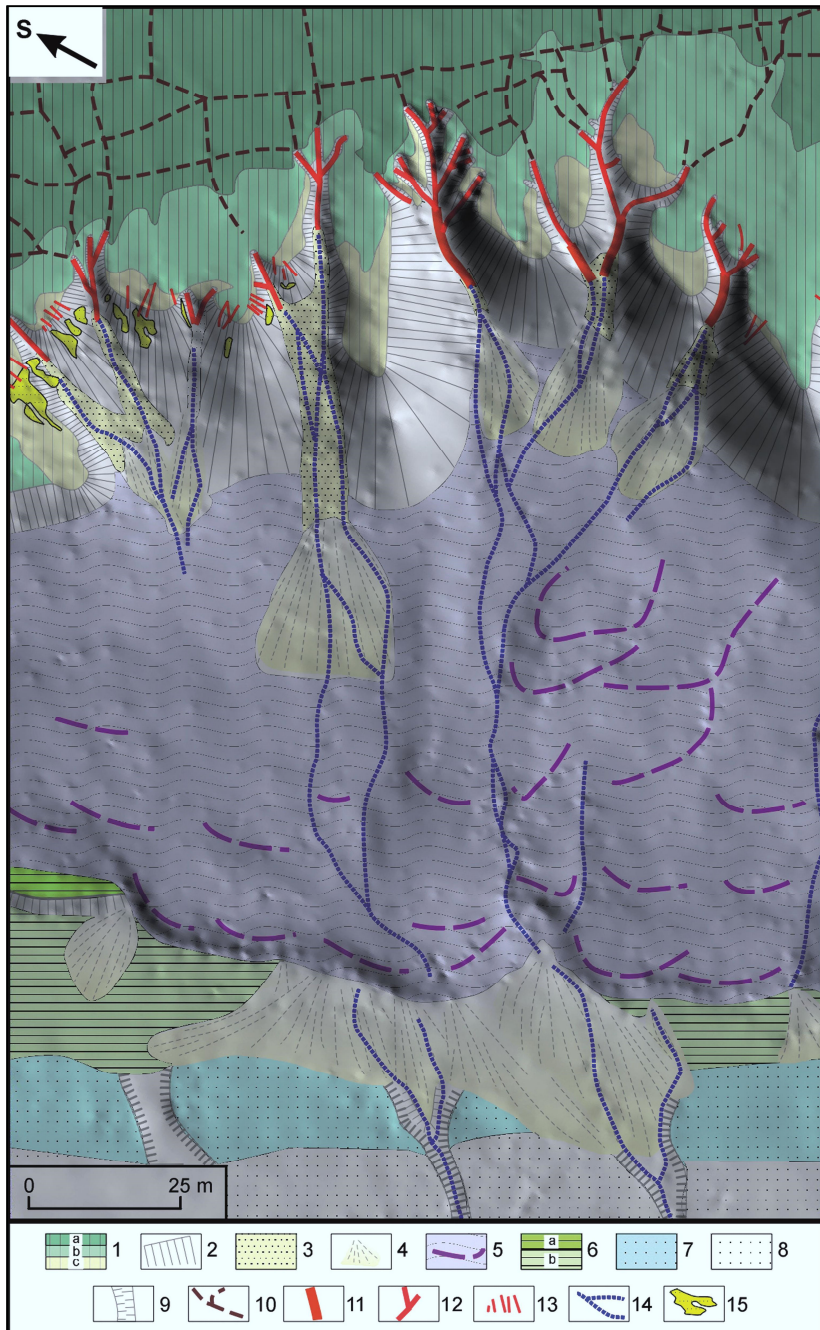


Fig. 5.3.13. Geomorphological sketch of dead cliff (E slope) (after: Superson & Zagórski 2008): 1- terrace III (22-30 m a.s.l.): a- dense vegetation, b- not dense vegetation, c- lack of vegetation, 2- slopes and erosional edges, 3- bottom of the flat-bottomed valley, 4- alluvial fans, 5- solifluction slope with lobes, 6- terrace I (2-8 m a.s.l.): a- older level, b- younger level, 7- the old storm ridge, 8- present-day storm ridge, 9- the cuts in present-day storm ridge, 10- thermal contraction cracks, 11- large V-shaped forms, 12- the medium-sized erosion rills, referring to the course of thermal contraction cracks, 13- small erosion rills, 14- the periodical stream channels, 15- the surface of sand-gravel accumulation.

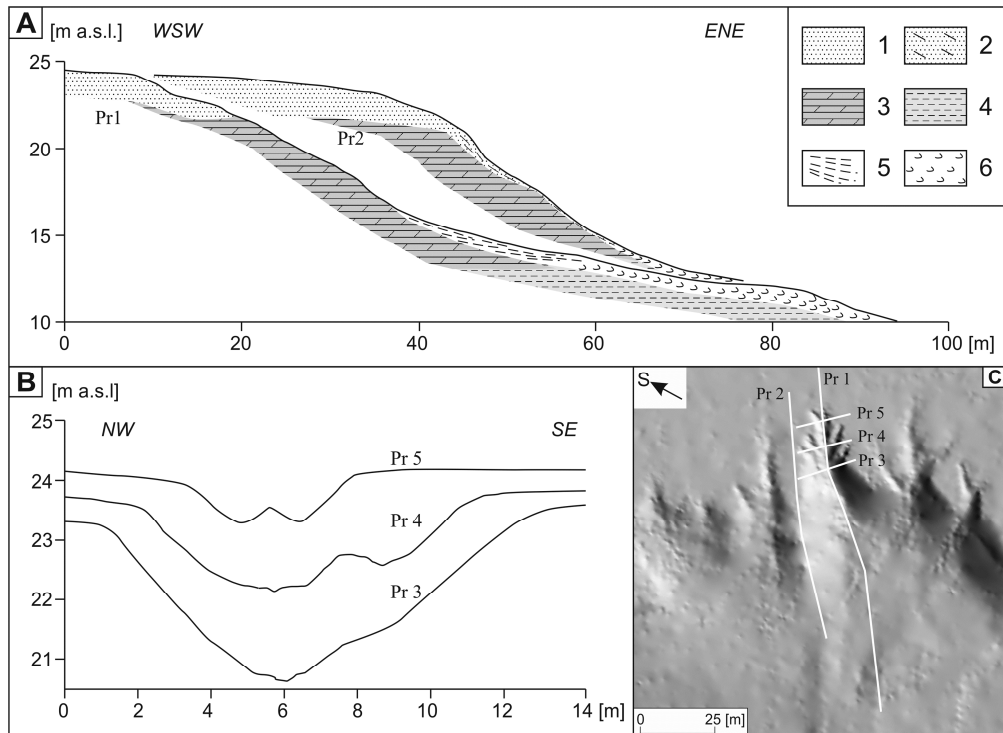


Fig. 5.3.14. Geological profiles by erosional forms norther part of study area (Superson & Zagórski 2008): A-longitudinal profiles: 1- marine gravels, 2- colluvial sands, 3- till, 4- marine clay, 5- alluvial fans, 6- solifluction covers; B-transverse profiles; C-location of profiles.



Photo 5.3.8. General view on marine terrace II edge cut by the erosion forms (Photo P. Zagórski 2006).

5.3. Permafrost and periglacial processes

Large, V-shaped erosion rills formed in the cohesive material of glacial till. The subsequent stage of development of these forms was the formation of flat-bottomed valleys (Fig. 5.3.13). These valleys formed due to the recession of the slopes under the influence of mass wasting and removal of colluvial material by periodic streams.

The progressing development of erosion forms leads to the recession of the highly inclined terrace slope towards the SW. The recession of the edge leaves a slightly inclined surface resting on marine clay while the material of erosional origin is accumulated in the form of alluvial fans. The impermeable clay causes the humidification of the terrain surface, which is conducive to intensive solifluction processes.

A characteristic feature of the landscape of river valleys and former sea bays are the ice-and-mineral mounds formed as a result of cryogenic processes in areas of occurrence of permafrost, and known by the Eskimo name **pingo**. Two genetic types of these forms are distinguished: the Greenland type, with an open system of water circulation, and the closed type (Mackenzie delta), with ground water freezing in the deltas and beneath the lakes (Jahn 1970).

Pingos occur in Dunderdalen which issues into the Greenland Sea, and within Chamberlindalen, close to where it opens onto Recherchefjorden (Figs. 5.3.15 and 5.3.16). A preliminary description of these forms was made by Liestøl (1976) who located them based on aerial photographs from 1960. They were also studied during several UMCS Polar Expeditions (Repelewsko-Pękalowa *et al.* 1987b; Pękala & Repelewsko-Pękalowa 2004, 2005).

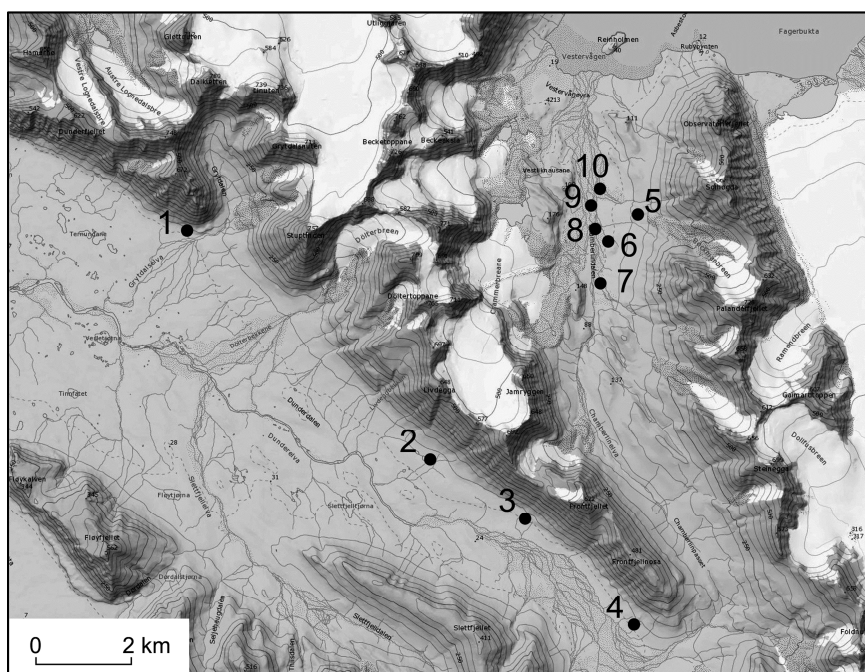


Fig. 5.3.15. Location of pingos in Dunderdalen and Chamberlindalen (Pękala & Repelewska-Pękalowa 2004). Background: Topo Svalbard, Norwegian Polar Institute.

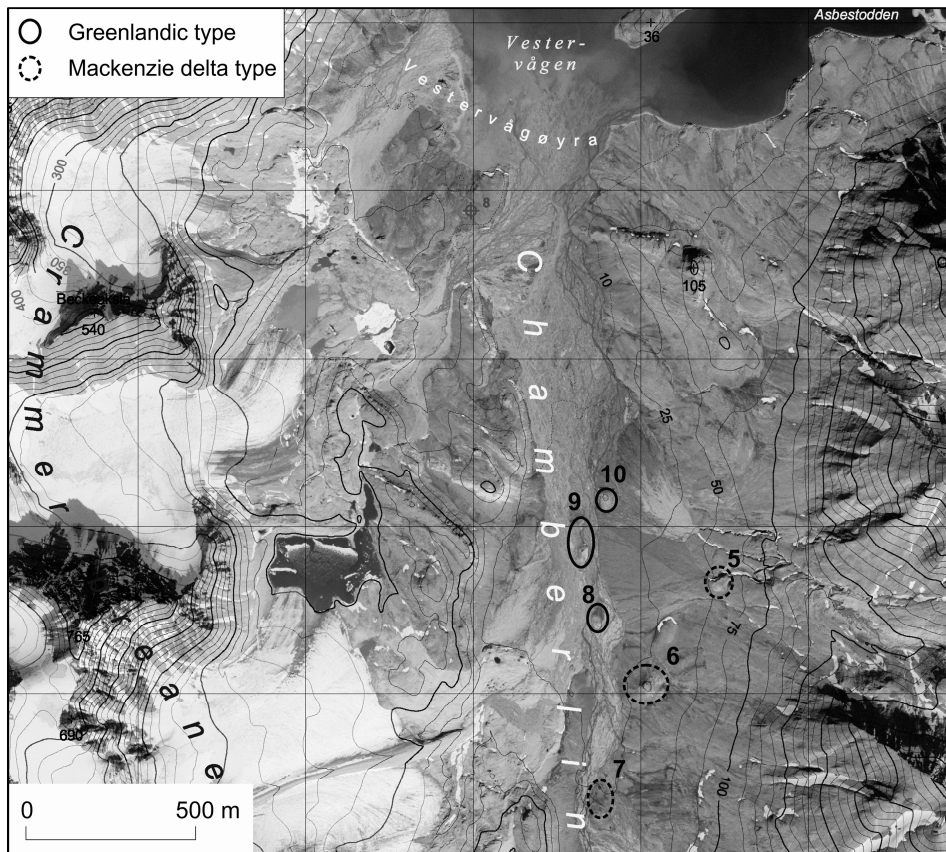


Fig. 5.3.16. Location of pingos in Chamberlindalen (Orthophotomap, Zagórski 2005).

There are four pingos of Greenlandic type in Dunderdalen (Fig. 5.3.15). One of them – pingo 2 – was situated at 40 m a.s.l., on the contact zone of shales and tillites with the slope deposits cover (Fig. 5.3.17, Photo 5.3.9). On the northern side of Lievdegg ridge there are firn fields of the subpolar Crammer glaciers. Pingo is of a vast cone shape, 30 m high and about 150 m diameter surrounded with a bar built of solifluction covers. The upper part of the cone is formed by gravelly-sandy deposits with chips and packs of limestones and tillites as well as green and grey shales. The presence of tectonic mirrors and strong mineralisation were found on larger blocks indicating the tectonic fault. Pingo is split: a contemporary active talus is put into a 60 m diameter crater. On its upper part there are gaping cracks, thermokarstic small lakes and water inflows from the contemporary craters. At the pingo foot and in the crater icing covers are formed in summer. Comparison of the morphological situation and the pingo shape in the aerial photographs made in the years 1960 and 1990, as well as the data from 2000, indicate the increasing activity of this form. Both the pingo foot zone and the upper part with the crater change (Pękala & Repelewska-Pękalowa 2004).

The second example of pingo Greenlandic type is object pingo 3. In this case two joined cones of a total diameter to 200 m, situated on a slightly sloped (3° - 7°) soli-

5.3. Permafrost and periglacial processes

fluction plain (Fig. 5.3.18, Photo 5.3.10). Solifluction covers accumulate on the forms, then pass them forming terraces and solifluction tongues directed to the valley axis. The high cone possesses an open crater in which a small lake with a bar on the border is situated. A dome of secondary pingo form was created in the crater of the small cone. Since 1986 no significant activities have been observed. Only the southern slopes undergo slow degradation due to solifluction.

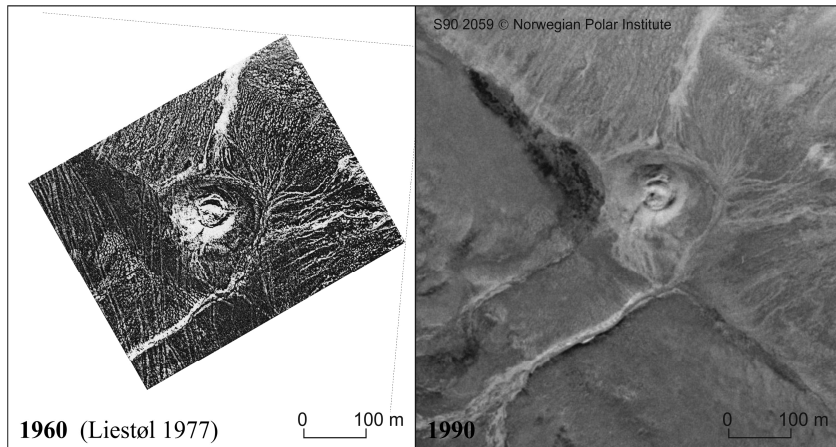


Fig. 5.3.17. Pingo 2 in Dunderdalen - Greenlandic type.



Photo 5.3.9. Pingo 2 in Dunderdalen - Greenlandic type (Photo K. Pękala 1989).

Pingos in Chamberlindalen occur within the delta plain, on alluvial fans and raised terraces. They represent various types in various stages of evolution. Pingos of the Greenland type developed in the ground where shale contacted the solid rock and in zones of tectonic relaxation, on raised terraces - up to 50 m a.s.l., forms 5, 6 and 7 (Fig. 5.3.16). The majority of these forms belong to the open Mackenzie delta type - forms 7-10 (Fig. 5.3.20, Photo 5.3.11). The youngest pingos, situated close to where the valley opens onto the Recherchefjorden, are oval mounds, 5-7 m high. The older pingos,

in the middle reaches of the valley, are higher (10-12 m). In the upper reaches of the valley, on a terrace at the eastern slope, the pingos are highly degraded, and some craters are filled with water. They even reach the height of 40 m. They formed in Quaternary deposits and correspond to the raised marine terraces 20-25 m, 10-12 m and 5-7 m (Pękala & Repelewska-Pękalowa 1988b).

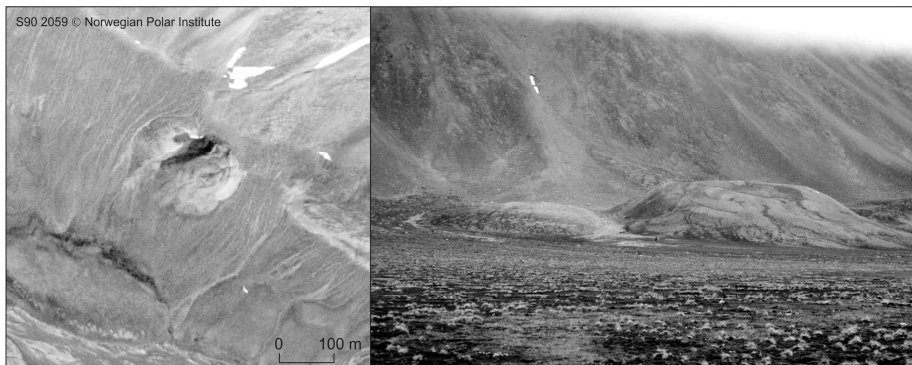


Fig. 5.3.18. Pingo 3 in Dunderdalen - Greenlandic type (Photo K. Pękala 1989).



Photo 5.3.10. Pingo 3 in Dunderdalen - Greenlandic type (Photo K. Pękala 1989).

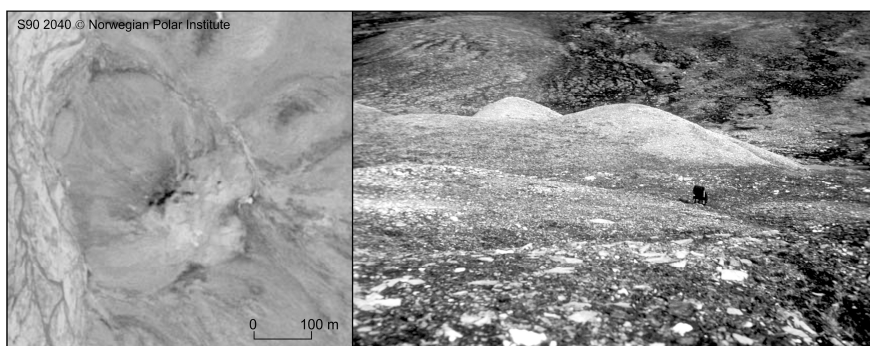


Fig. 5.3.19. Pingo 6 in Chamberlindalen - Greenlandic type (Photo K. Pękala 1987).

5.3. Permafrost and periglacial processes

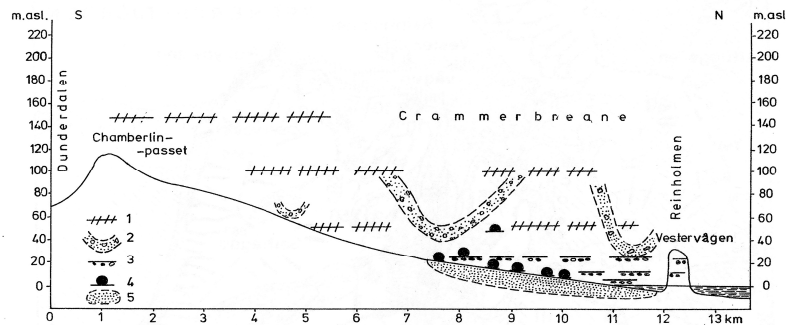


Fig. 5.3.20. Longitudinal profile of the Chamberlindalen and main relief elements (Pękala-Repelewska-Pękalowa 1988b): 1- structural levels and marine terraces, 2- extents of the frontal moraines, 3- marine terraces with accumulative cover, 4- pingo, 5- Quaternary deposits (marine and delta origin).

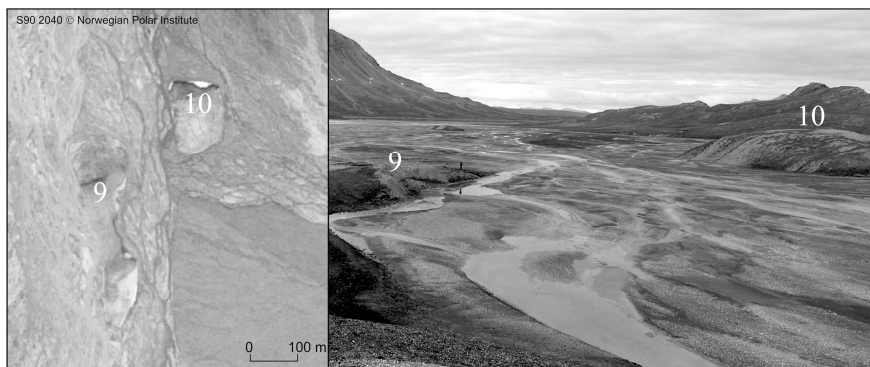


Fig. 5.3.21. Pingos 9 and 10 in Chamberlindalen - Mackenzie delta type (Photo P. Demczuk 2009).



Photo 5.3.11. Pingos 8, 9 and 10 in Chamberlindalen - Mackenzie delta type (Photo P. Zagórski 2005).

Observations conducted during the investigations in Dunderdalen and Chamberlindalen confirm the previous views on the processes and mechanisms of the development of pingo forms of the open and closed type. These forms are in various stages of development and current activity. Their distribution, dependent on geological structure and relief, indicates a link with the migration of water from source areas (subpolar glaciers and water overlying permafrost).

Streszczenie

Wieloletnia zmarzlina i procesy peryglacialne

Spitsbergen leży w zasięgu występowania w podłożu wieloletniej zmarzliny ciągłej (*permafrost*), której miąższość osiąga nawet 450 m. W dodatniej temperaturze powietrza w okresie polarnego lata rozmarza jej strop i formuje się tzw. warstwa czynna. Budowa geologiczna, a zwłaszcza rodzaj utworów pokrywowych, ukształtowanie powierzchni topograficznej, obecność wód na powierzchni i ich krążenie w obrębie czynnej warstwy zmarzliny sprzyjają działalności procesów geomorfologicznych, charakterystycznych dla warunków peryglacialnych, takich jak: soliflukcja, spłukiwanie, spływy błotne, osuwanie, segregacja i pęcznienie mrozowe, wietrzenie mrozowe, termoerozja oraz erozja linijna. Pomiary miąższości warstwy czynnej oraz ruchu soliflukcyjnego prowadzono w okresie 1986-2009 w obrębie charakterystycznych ekosystemów tundry, zróżnicowanych pod względem obecności wody w pokrywach i stopnia jej mobilności, nachylenia powierzchni i jej ekspozycji oraz rodzaju pokrywy roślinnej. Maksymalne wielkości letniego rozmarzania wały się w granicach od 40 cm do ponad 225 cm (tabela 5.3.1). Najmniejsze wartości notowano na stanowisku z wodą stojącą na powierzchni (małe, płytkie jeziorko tundrowe), zaś największe – na powierzchniach nachylonych, gdzie woda w gruncie była w ruchu, odgrywając rolę nośnika ciepła. Wyniki te, uznane za reprezentatywne dla obszarów leżących w zasięgu wpływów północnego Atlantyku, zostały włączone, jako Site P1 – Calypsostranda, do międzynarodowego programu CALM (*Circumpolar Active Layer Monitoring*), koordynowanego przez International Permafrost Association (IPA). Wiodącą rolę wśród procesów peryglacialnych odgrywa soliflukcja. Pomiary ruchu soliflukcyjnego prowadzono różnymi metodami, w tym od roku 2006, przy użyciu odbiorników geodezyjnych GPS (Leica, system 500). Tempo tego ruchu było bardzo zróżnicowane, od 2,1 cm·rok⁻¹ (stok N) do 53,3 cm·rok⁻¹ (stok S). Skutkiem morfologicznym soliflukcji jest powstawanie niszących, małych cyrków i niecek oraz jazorów błotnych i gruzowych. Stwierdzono istnienie wielu form charakterystycznych dla obszarów występowania wieloletniej zmarzliny, takich jak: grunty strukturalne, żyły, soczewy i kliny lodowe, a także lodowo-mineralne pagórki pinga (zarówno typu otwartego, jak i zamkniętego) oraz dolinki erozyjne (ryc. 5.3.1, fot. 5.3.1). Wzrost aktywności procesów peryglacialnych, obserwowany od roku 2000, świadczy o reakcji wieloletniej zmarzliny na rejestrowane zmiany klimatu.

Objaśnienia

Ryciny

Ryc. 5.3.1. Główne formy i lokalizacja punktów pomiarowych czynnej warstwy zmarzliny (Repelewska-Pękalowa, Pękala 2003): 1- plaża, 2- dna dolin i strefy stożków aluwialnych u podstawy klifu, 3- klif i krawędzie erozyjne dolin, 4- suche powierzchnie teras morskich, 5- strefy aktywnej soliflukcji, 6- okresowo wilgotne terasy ze stożkami aluwialnymi, 7- zbocza i wysokie terasy morskie przekształcane przez procesy wietrzenia, krioplanacji i erozji, 8- okresowe jeziorko, 9- rozcięcia erozyjne, 10- punkty pomiarowe i profile.

Ryc. 5.3.2. Plan i profile potoku błotnego na stoku martwego klifu terasy 20-25 m n.p.m. w Calypsobyen (Pękala 2004).

Ryc. 5.3.3. Plan i przekroje błotnistego cyrku (nisza) z jezorem soliflukcyjnym (Pękala 2004).

Ryc. 5.3.4. Położenie badanych stoków (DEM, Zagórski 2002).

Ryc. 5.3.5. Ruch soliflukcyjny na stoku o ekspozycji wschodniej w latach 2006-2009.

Ryc. 5.3.6. Ruch soliflukcyjny na stoku o ekspozycji zachodniej w latach 2006-2009.

Ryc. 5.3.7. Ruch soliflukcyjny na stoku o ekspozycji północnej w latach 2006-2009.

5.3. Permafrost and periglacial processes

- Ryc. 5.3.8. Ruch soliflukcyjny na stoku o ekspozycji południowej w latach 2006-2009.
- Ryc. 5.3.9. Ruch soliflukcyjny na stoku o ekspozycji północno-wschodniej w latach 2006-2009.
- Ryc. 5.3.10. Rozwój wieńców kamienistych (Pękala 2004, fot. S. Bartoszewski 2002).
- Ryc. 5.3.11. Etapy rozwoju struktur segregacji mrozowej na powierzchni moreny dennej z jądrem martwego lodu - przedpole Renardbreen (Pękala 2004).
- Ryc. 5.3.12. Plan i stadia rozwoju form sufozyjnych (Repelewska-Pękalowa 1996).
- Ryc. 5.3.13. Szkic geomorfologiczny fragmentu martwego klifu Calypsostrandy (Superson, Zagórski 2008): 1- terasa III (22-30 m n.p.m.): a- zwarta roślinność, b- niezwarta roślinność, c- brak roślinności, 2- stoki i krawędzie erozyjne, 3- dna form płaskodennych, 4- stożki napływowie, 5- stok soliflukcyjny, loby soliflukcyjne, 6- terasa I (2-8 m n.p.m.): a- poziom starszy, b- poziom młodszy, 7- stary wał sztormowy, 8- współcześnie kształtowany wał sztormowy, 9- rozcięcia w obrębie wałów sztormowych, 10- przebieg szczelin kontrakcji termicznej, 11- duże V-kształtne formy, 12- średnie bruzdy erozyjne, nawiązujące do przebiegu struktur kontrakcji termicznej, 13- małe bruzdy erozyjne, 14- koryta potoków okresowych, 15- powierzchnie akumulacji piaszczysto-żwirowej.
- Ryc. 5.3.14. Przekroje geologiczne i formy erozyjne północnej części badanego obszaru: A- profile podłużne: 1- żwiry morskie, 2- piaski koliwialne 3- glina zwałowa, 4- ilły morskie, 5- stożek napływowi, 6- soliflukcja; B- profile poprzeczne; C- lokalizacja profilów.
- Ryc. 5.3.15. Lokalizacja pagórków pingo w Dunderdalen i Chamberlindalen (Pękala, Repelewska-Pękalowa 2004). Podkład: Topo Svalbard, Norwegian Polar Institute
- Ryc. 5.3.16. Położenie pagórków pingo w Chamberlindalen (Orthophotomap, Zagórski 2005).
- Ryc. 5.3.17. Pingo 2 w Dunderdalen – typ grenlandzki.
- Ryc. 5.3.18. Pingo 3 w Dunderdalen – typ grenlandzki (fot.K. Pękala 1989) .
- Ryc. 5.3.19. Pingo 6 w Chamberlindalen – typ grenlandzki (fot. K. Pękala 1987).
- Ryc. 5.3.20. Profil podłużny Chamberlindalen i główne elementy rzeźby (Pękala, Repelewska-Pękalowa 198b): 1- poziomy strukturalne i terasy morskie, 2- zasięgi moren czołowych, 3- terasy morskie z pokrywą akumulacyjną, 4- pingo, 5- osady czwartorzędowe (morskie i deltowe).
- Ryc. 5.3.21. Pinga 9 i 10 w Chamberlindalen – typ Mackenzie delta (fot. P. Demczuk 2005).

Fotografie

- Fot. 5.3.1. A- intensywne procesy soliflukcji powyżej budynku – Calypsobyen (fot. K. Pękala 2005), B- nisza z jęzorem soliflukcyjnym (fot. P. Zagórski 2010).
- Fot. 5.3.2. Pomiar GPS: A- na stoku o ekspozycji wschodniej (fot. P. Zagórski 2006), B- na stoku o ekspozycji zachodniej (fot. P. Zagórski 2009).
- Fot. 5.3.3. Pomiar GPS: A- na stoku o ekspozycji północnej (fot. P. Zagórski 2009), B- na stoku o ekspozycji południowej (fot. P. Zagórski 2006).
- Fot. 5.3.4. Pomiar GPS na stoku o ekspozycji północno-wschodniej (fot. P. Zagórski 2006).
- Fot. 5.3.5. A,B- efekty zmywu powierzchniowego na krawędzi podniesionej terasy II, Calypsobyen (fot. P. Zagórski 2006).
- Fot. 5.3.6. Formy segregacji mrozowej na powierzchni Calypsostrandy w pobliżu Tyvjobekken (Potok Wydrzycy) (fot. K. Pękala).
- Fot. 5.3.7. Przykłady procesu termoerozji: A- w pobliżu Beisodden (fot. S. Bartoszewski 2001), B- w pobliżu Beisodden (fot. M. Świtoniak 2009), C- degradacja klinów mrozowych na Reinslettice (fot. K. Pękala 2000).
- Fot. 5.3.8. Ogólny widok krawędzi terasy III z formami erozyjnymi (fot. P. Zagórski 2006).
- Fot. 5.3.9. Pingo 2 w Dunderdalen – typ grenlandzki (fot. K. Pękala 1989).
- Fot. 5.3.10. Pingo 3 w Dunderdalen – typ grenlandzki (fot. K. Pękala 1989).
- Fot. 5.3.11. Pinga 8, 9 i 10 w Chamberlindalen – typ Mackenzie delta (fot. P. Zagórski 2005)

Tabele

Tabela 5.3.1. Letnie rozmarzanie czynnej warstwy zmarzliny w różnych punktach Calypsostrandy w okresie 1986-2012 (wielkości maksymalne – w cm).

Tabela 5.3.2. Tempo soliflukcji w rejonie Calypsostrandy na zboczach o różnej ekspozycji w określonej 1987-1991 (Repelewska-Pękalowa, Pękala 1993).